INTERNATIONAL RESEARCH JOURNAL OF ENGINEERING & APPLIED SCIENCES
ISSN: 2322-0821(O) ISSN: 2394-9910(P)
VOLUME 14 ISSUE 1 Jan 2026 - Mar 2026
www.irjeas.org

*Research Article*

# Microstructure Refinement and Mechanical Isotropy Enhancement in WAAM Ti–6Al–4V via Interpass Rolling

**Anil Sharma [1]*, Dr. Alok Choudhary [2]**

[1]*Research Scholar, Department of Mechanical Engineering Dr. A P J Abdul Kalam University, Indore
anilsharma2909@gmail.com
[2]Assistant Professor, Department of Mechanical Engineering Dr. A P J Abdul Kalam University, Indore
dr.alokchoudhary@aku.ac.in

*Corresponding Author: anilsharma2909@gmail.com
DOI–10.55083/irjeas.2026.v14i01004



**Abstract:** Wire Arc Additive Manufacturing (WAAM) of Ti-6Al-4V allows bulk structural elements to be manufactured at high rates of deposition, but carries the inherent costs of coarse columnar prior- Β grains and high mechanical anisotropy, because of directional solidification, and repeated thermal cycling. Interpass rolling is used in this study as an in-situ thermo-mechanical processing method to improve microstructure and mechanical isotropy in Ti-6Al-4V fabricated by WAAM. Rolling loads of 50 and 75 kN were carried out using flat and profiled rollers in deposition and their impact on the evolution of the microstructure and tensile behavior was studied systematically. Optical microscopy, SEM, and EBSD microstructural characterization indicate a high degree of refinement of prior-β grains (≈20–25%) and narrowing of the α-lath width to approximately ~10 μm with the increasing severity of rolling, especially in the roller being profiled (75 kN). Interpass rolling also suppresses heat-affected zone banding and interrupts columnar continuity of β-grain. A tensile test in the build (Z) and the transverse (X) directions shows that mechanical anisotropy can be reduced significantly, with the difference in the strengths being reduced by more than ~35 MPa in the unrolled form to less than 10 Mpa after rolling. The synergistic strengthening, ductility and isotropy are explained by strain-assisted recrystallization and homogenization of microstructure caused by interpass rolling. These results make interpass rolling an interesting strategy to manufacture mechanically isotropic WAAM Ti–6Al–4V parts, without the necessity of post-deposition thermomechanical processing and hence scaled.

**Keywords: Wire Arc Additive Manufacturing (WAAM), TIG-based additive manufacturing, Ti–6Al–4V titanium alloy, process parameter optimization, bead geometry control, layer height and width, heat input per unit length, melt pool**

**dynamics, transient thermal finite element modelling, and empirical regression modelling.**

## 1. INTRODUCTION

Wire Arc Additive Manufacturing (WAAM) has become an additive manufacturing (AM) process based on directed energy deposition (DED) with large scale titanium alloy parts exhibiting high deposition rates and less material waste. Ti–6Al-4V is the most common of titanium alloys due to its high specific strength, corrosion resistance, and good performance of aerospace and biomedical applications. Nevertheless, in spite of these benefits, WAAM-produced Ti-6Al-4V parts typically exhibit coarse columnar prior- β grains, significant texture and high-level mechanical anisotropy, which restricts their structural integrity and increased industrialization.

Directional solidification under steep thermal gradient and repeated thermal cycling when depositing layer-by-layer is what results in the inherent anisotropy of WAAM. This gives long columnar β grains oriented parallel to the build direction and lamellar α/β microstructure whose morphology is spatially varied in the deposit. The same microstructure-property relationships have been observed in DED-based processes, where process parameters have a significant effect on the geometry of the melt pool, grain structure, and phase development (Narra et al., 2018; Narayana et al., 2021). Although density and geometry can be partially controlled by optimization of processing parameters like power, scan speed and feed rate, microstructural anisotropy is hard to get rid of by thermal control alone.

The problem of mechanical anisotropy of titanium alloys is known to be a significant issue, as it directly influences the strength in the form of the yield, ductility, and fracture behavior at various orientations. Lei et al. (2021) have shown that anisotropy in titanium alloys is a result of deformation texture, slip-activated, and morphology, which results in yielding and plasticity that is direction dependent. In additively manufactured Ti -6Al -4V, these effects are worsened by the columnar grain structure of fibrous nature formed during deposition, which leads to poor mechanical performance in the build direction as opposed to the transverse direction.

To overcome these shortcomings, a number of post-processing techniques including heat treatment, hot isostatic press (HIP) and hybrid processing pathways have been examined. It has been demonstrated that hybrid processes involving WAAM followed by subsequent hot deformation or forging can be promising in the minimization of texture content, the establishment of dynamic recrystallization, and isotropy (Maurya et al., 2022). Nevertheless, these methods tend to be more processing intensive, higher temperature, and need complicated tooling that inflates costs of production and lowers the efficiency of manufacturing.

Recently, interpass rolling has been interesting in as powerful in situ thermo-mechanical treatment of WAAM processes. Interpass rolling implants plastic deformation on the newly solidified material by putting the deposited layers through mechanical deformation when the material is still thermally active. This strain concentration facilitates strain-enhanced recrystallization in the later thermal treatments hence inhibiting columnar β-grain thriving and increasing the microstructural uniformity. Interpass rolling in comparison to post-deposition deformation has the benefit of smoothly becoming part of the WAAM process chain since microstructure control during fabrication can be achieved without any further high-temperature processing.

It has been demonstrated in previous research that the additive manufacturing controlled deformation can have a significant impact on grain refinement and texture development. The study of Narra et al. (2018) revealed that even the pre-existing β-grain width in Ti-6Al-

4V scales is very sensitive to the melt pool geometry, which shows that microstructure is highly sensitive to local thermal -mechanical conditions. In the same manner, hybrid WAAM-forging research has validated that the addition of deformation enhances texture and strengthens and ductile strength with fined and equiaxed microstructures (Maurya et al., 2022). Such results suggest that mechanical intervention during or right after deposition is an effective method of microstructure and property personalization.

Nevertheless, the systematic studies of interpass rolling load and roller geometry effects on microstructure refinement and mechanical isotropy in WAAM Ti 6Al 4V are still incomplete. Specifically, the correlation between rolling-induced β-grain fragmentation, $\alpha$-lath refinement, and tensile anisotropy reduction across the build and transverse directions has not been completely measured. In addition, the behaviors of various roller geometries on strain distribution and recrystallization should be known to optimize the interpass rolling strategy.

Thus, this research will explore how interpass rolling can influence the development of microstructure and mechanical isotropy in Ti–6Al 4V fabricated by WAAM. The rollers used were flat rollers and profiled rollers under varying rolling loads to investigate their effect on the previous stages of β -grain refinement, $\alpha$-lath structure, and heat-affect zone banding in a systematic manner. Anisotropy reduction was measured by the mechanical performance of tensile testing in the build (Z) and transverse (X) directions. This work proves that interpass rolling is a promising and scalable method of improving mechanical isotropy and structural reliability in WAAM Ti -6Al -4V components by demonstrating direct correlations between microstructure and property.

## 2. LITERATURE REVIEW

### 2.1 Microstructural Anisotropy in WAAM Ti–6Al–4V

The high heat input and directional solidification of Critical Arc Additive Manufacturing (WAAM) of Ti-6Al-4V is known to form coarse columnar prior- β grains that run along the build direction and a powerful ⟨001⟩ β-fiber texture. Martina et al. (2015) have shown that these columnar grains can cut across the entire thickness of the wall, and result in repetitive Widmanstätten $\alpha$-lamellar colonies, and high levels of microstructural heterogeneity. These characteristics are generally known to be the main microstructural source of mechanical anisotropy in WAAM titanium alloys.

McAndrew et al. (2018) also stated that uninterrupted growth of epitaxial β-grains is encouraged by the laterally constrained geometry of WAAM, especially in thick walls and intersecting features. The resulting elongation of the grains and high texture directly affects the strain localization and deformation behavior which reduces isotropic mechanical behavior. Such results define microstructural anisotropy as an inherent constraint of traditional WAAM processing pathways of Ti 6Al 4V.

### 2.2 Rolling of Interpass as an In-Process Microstructure Control Strategy.

High-pressure interpass rolling has proved to be among the most effective in-process strategies in order to reduce columnar β-grain growth in WAAM Ti -6Al-4V. One of the first systematic studies of the impact of interpass rolling was given by Martina et al. (2015) who showed the presence of centimeter-scale columnar β grains and refined equiaxed grains with a diameter between 56 to 139 μm. Their analysis has pointed out that flat as well as profiled rollers can cause extensive grain refinement, even though profiled rollers yielded more effective interference with columnar grain continuity.

Based on this background, McAndrew et al. (2018) proposed an inverted profiled roller to be used on complicated WAAM geometries. They demonstrated, with the EBSD analysis, that the rolling strain that was applied is not evenly distributed, with the greatest strain concentrated along the edges of the groove and along a distance of about 3 mm below the rolled surface. Notably, they showed that the addition of rolling load and roller radius enlarges the recrystallized zone which results in a more uniform grain size distribution across the layer deposited.

### 2.3 Strain Localization, Recrystallization and Grain Refinement Processes.

A sophisticated technique of EBSD-based strain mapping has helped in elucidating the mechanistic foundation of the process of grain refinement occasioned by interpass rolling. Davis et al. (2020) devised a large-area SEM-based local average misorientation (LAM) calibration method of measuring effective plastic strain in interpass rolled WAAM Ti6Al4V. Their findings showed that there was a good spatial relationship between areas of elevated plastic strain with consequent β -grain recrystallization on rapid heating via the β -transus. The greatest measurable strain was close to the value of about 12% and then LAM saturation was reached.

Donoghue et al. (2020) also added some complementary information to the dataset as they utilized in-situ EBSD and synchrotron X-ray diffraction to prove that the refinement of grains in interpass-deformed WAAM Ti-6Al-4V is not only deformation-driven but highly dependent on annealing twinning in the process of β-grain regrowth. They discovered a distinctive four-pole β-texture motif produced by the process of double twinning in rapid thermal cycling, an AM-specific process.

### 2.4 Effect of Microstructural Refinement on Mechanical Behavior and Isotropy.

Full-field strain analysis has been used to determine the relationship between refined microstructure and mechanical response. Lunt et al. (2020) established that unrolled WAAM Ti-6Al-4V has a very heterogeneous strain localization during tensile loading, especially when subjected to tensile loading that is normal to the columnar β-grain direction. This was associated with the existence of dominant hard and soft $\alpha$ icons in large β grains. It was demonstrated that the interpass rolling can evenly redistribute the strain in all loading orientations, which demonstrates its efficiency in avoiding the anisotropy of deformation.

Similar results have been obtained with other in-process deformation processes. As demonstrated by Hönnige et al. (2020) and Xian et al. (2024), machine hammer peening may decrease average β-grain size of centimeter size down to less than 0.5 mm and diminish strength of texture significantly. Xian et al. (2024) also reported a decrease in tensile anisotropy which were correlated to the spatial distribution of plastic strain (MAX–MED–MIN zones) and previous-β grain morphology.

Similar trends have also been seen in micro-rolling in plasma arc additive manufacturing. According to Pan et al. (2022), interpass micro-rolling led to a decrease in the defect density, refinement of $\alpha$-lath morphology, and decrease in the mechanical anisotropy, which produced increase in strength and ductility both along build and transverse orientations.

## 3. METHODOLOGY

### 3.1 WAAM Fabrication and Interpass Rolling

The Ti -6Al-4 V walls were made by wire arc additive manufacturing (WAAM) on the basis of tungsten inert gas (TIG). The deposition was done in layer-by-layer controlled deposition so that the arc would behave in a stable way and that the beads would have their geometry in a consistent way. The orientation of building was set in a way that the deposition direction was parallel to the transverse (X), where the build height was parallel to the vertical (Z) direction.

The interpass rolling was used as an in-situ treatment that involved thermo-mechanical treatment before further deposition of the layer on top. A rolling was done in the presence of a thermally active material that was deposited and the rolling allowed effective plastic deformation and the build-up of strain in the newly deposited layers.

The two geometries have been explored which include a flat roller and a profiled roller. The rolling loads of 50 kN and 75 kN were determined using the literature-reported literature deformation thresholds of Ti -6Al -4V fabricated using the WAAM method. The rolling load of 100 kN was studied firstly, but sooner the fracture took place due to overstrain accumulation, when deposition reached the seventh layer. This condition was thus not subjected to any further characterization so as to offer consistency and comparability across samples.

The substrate used in the WAAM was a Ti-6Al-4V base plate that was 405 x 60 x 6 mm3. To fix the base plate to the build platform, mechanical fasteners were used in order to prevent movement to the side and to maintain the same contact between roller and deposited material when rolling.

### 3.2 Microstructural Characterization

Microstructural characterization was done to determine the effect of rolling load and roller geometry on grain refinement, phase morphology and microstructural homogeneity.

Macrostructural characteristics (previously- β -grain morphology and heat-affected zone (HAZ) banding) were observed under optical microscopy (OM). Standard procedures applicable to Ti–6Al–4V alloys were used to section the metallographic specimens transverse to the direction of the build, mount, polish and etch.

Higher magnifications of microstructural features were studied under the scanning electron microscopy (SEM), such as $\alpha$-lath morphology, β-grain fragmentation and grain boundary characteristics. SEM imaging allowed paying detailed attention to refinement levels being attained in various rolling conditions.

In the selected samples, electron backscattered diffraction (EBSD) was performed to compare β -grain orientation, continuity of grain boundaries, and degree of grain fragmentation caused by interpass rolling. Inverse pole figure (IPF) maps were created to evaluate the changes in crystallographic texture and build-direction anisotropy.

Quantitative measurements of $\alpha$-lath width and prior β-grain size were performed using ImageJ image analysis software. Multiple micrographs were analyzed for each condition to ensure statistical reliability, and average values were reported for comparative analysis.

To examine the phase constitution and ensure the absence of phase transformations through deformation (rolling) of the samples, X-ray diffraction (XRD) was conducted on representative samples. Since no additional phase shifts were observed, no additional discussion of the XRD results is provided.

### 3.3 Tensile Testing

The mechanical properties were tested in terms of uniaxial tensile test at room temperature. Tensile samples were removed in the WAAM-built walls in two orientations: transverse (X) direction; that is, perpendicular to the deposition path, and build (Z) direction; that is, perpendicular to the build height. In this way, quantitative determination of mechanical anisotropy linked to the process of layer-by-layer deposition became possible.

Sub-size tensile specimens were machined to additive appropriate geometries of components. Gauge length of 24 mm and overall length of 27 mm were used in each specimen, and care was observed during machining to ensure that surface defects and edge damage which would affect tensile response would be minimized.

Tensile tests were realized under the displacement control with a universal testing machine. Strain measurement was done on non-contact laser extensometer to make it very accurate and to avoid errors caused by compliance of the grip or slippage of specimen. Each condition was found to have yield strength (0.2% offset), ultimate tensile strength (UTS), and elongation to failure.

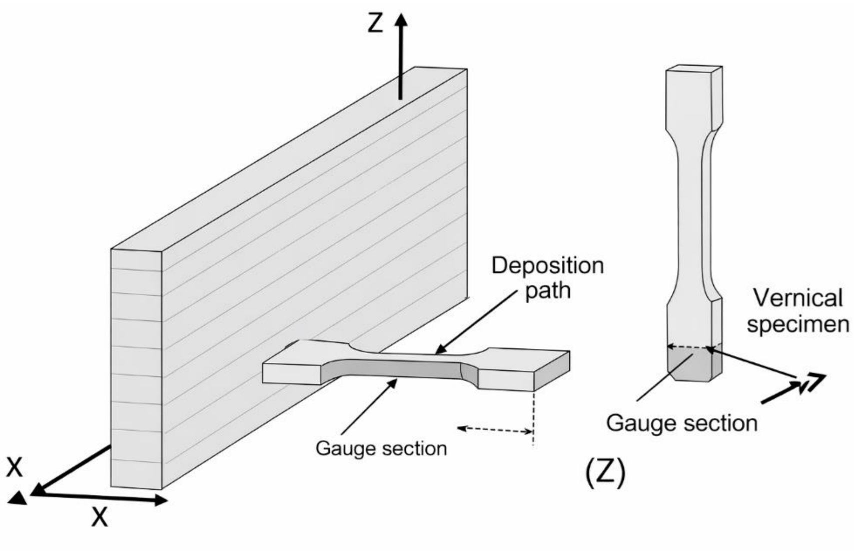


**Figure 1. Tensile specimen extraction orientations from WAAM wall**

### 3.4 Control of Oxygen Content

All experiments were done in an enclosed argon chamber to reduce oxidation in deposition and interpass rolling. In the process, oxygen levels in the enclosure were kept at levels of less than 4000 ppm. Besides arc shielding, a trailing shielding system was also used to secure the molten pool and the recently solidified material.

Oxygen content of the chosen samples was determined by the LECO oxygen analyzer to confirm that interpass rolling did not cause the significant oxygen uptake. The findings showed that the level of oxygen was maintained within reasonable ranges, which meant the observed alteration in the microstructure and mechanical properties was mainly due to microstructural modification caused by rolling, but not by compositional difference.

## 4. RESULTS AND DISCUSSION

### 4.1 Microstructural Evolution during WAAM and Interpass Rolling

Directional solidification repeated thermal cycling and mechanically induced strain due to inter pass rolling are the determinants of microstructure of Ti-6Al-4V fabricated using WAAM. A methodical comparison of the as-deposited and rolled states indicate the usefulness of rolling in the inhibition of microstructural heterogeneity as well as minimization of build-direction anisotropy.

#### 4.1.1 As-Deposited Microstructure

The as deposited WAAM Ti-6Al-4V has a highly anisotropic microstructure characteristic of arc based additive manufacturing. Optical and SEM images (Fig. 2a, b, c) display coarse columnar prior- β grains which cross cut various deposited layers through the build (Z) direction. The morphology is formed due to the solidification under steep thermal fields and unidirectional heat flux between the mater pool and the substrate and the already deposited materials.

An $\alpha/\beta$ microstructure, which is lamellar, is found in the columnar prior- beta grains, composed of $\alpha$-lath that are enclosed within a retained β-microstructure. The thickness of $\alpha$-lath changes spatially with the local cooling rates where lamellae in areas with lower cooling rates will be coarser. This results in the free zone of mechanical deformation during deposition, and therefore, continuous growth of β-grains, which results in a low density of grain boundaries and strong microstructural anisotropy.

One of the typical aspects of as-deposited condition is that it exists in the form of the banding of heat-affected zone (HAZ), which is visible in the form of other microstructural layers oriented perpendicular to the direction of the deposition (Fig. 2b). These are the bands obtained by reheating of already deposited layers to temperatures near or even higher than the 8(3) -transus, and this is followed by some β-reversion and β-re-precipitation. These types of banding create microstructural discontinuities across the build direction and have been shown to cause scatter in the mechanical properties and decreased build-direction ductility.

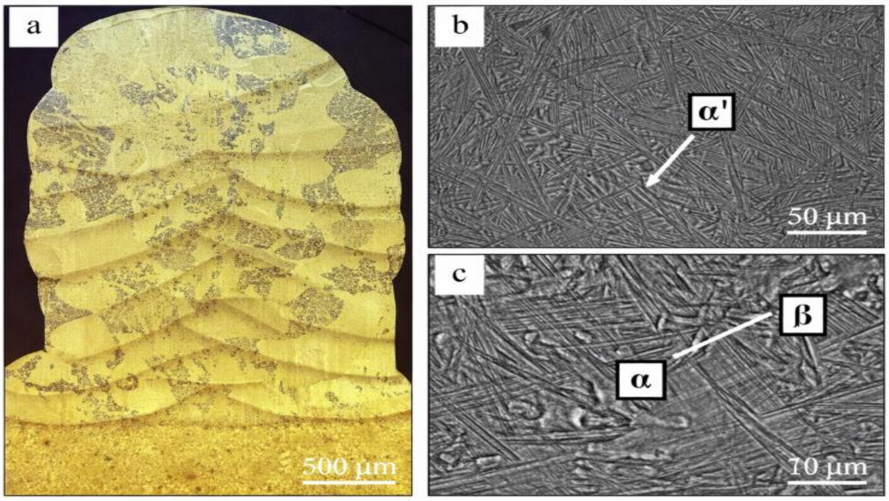


**Figure 2(a-c) As-deposited microstructure of WAAM-fabricated Ti–6Al–4V alloy. (a) Optical macrograph showing large columnar prior-β grains extending across multiple deposited layers along the build direction, indicative of epitaxial grain growth under directional heat flow. (b) SEM micrograph revealing acicular $\alpha'/\alpha$ lamellar colonies formed due to rapid cooling during WAAM deposition. (c) High-magnification SEM image showing coarse $\alpha$-laths and retained β phase, reflecting limited microstructural refinement in the absence of interpass rolling**

### 4.1.2 Effect of Interpass Rolling on Grain Refinement

There is a significant change on the WAAM microstructure due to interpass rolling. SEM and EBSD analyses (Fig. 3a -c) show that prior-β grain size is evidently reduced and the continuity of columnar grains in all the rolled conditions is disrupted compared to the unrolled one.

Rolling imparts plastic strain in the fresh deposited layers, and builds with the increasing rolling load. Such strain energy is stored, and encourages the formation of recrystallization as the next thermal cycles occur as a result of further deposited layers. Consequently, the columnar β grains are refined into equiaxed grains, which are smaller in size; the degree of refinement highly depends on the rolling load and roller geometry.

Partial grain refinement is obtained at a rolling load of 50 kN, which is localized continuity of columnar β-grains. Addition of the rolling load to 75 kN causes great refinement, and profiled rollers give the homogeneous and refined microstructure. It is the non-uniform contact geometry of the profiled roller that contributes to its increased effectiveness because it produces elevated localized plastic strain relative to a flat roller with the same nominal load.

Besides β -grain refining, interpassing that takes place during the process of rolling results in significant thinning of the 3rd β -grain (a-lath). It can be found that the average $\alpha$-lath width reduces to about 1518 mm in the unrolled status to around ~10–12 µm in samples rolled at the 75 kN with a profiled roller (Fig. 3c). Additionally, the intensity of HAZ banding is significantly low, which means enhanced microstructural consistency along the build height.

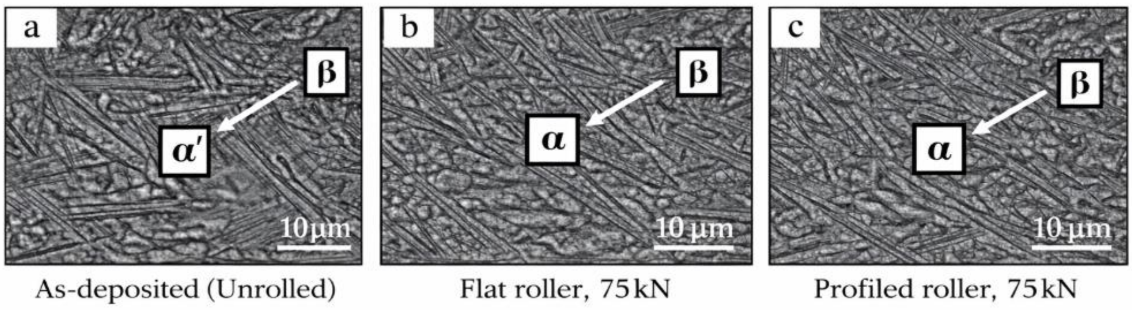


**Figure 3(a-c) Scanning electron microscopy (SEM) images comparing $\alpha$-lath morphology in WAAM Ti–6Al–4V: (a) as-deposited (unrolled) condition, (b) interpass rolled using a flat roller at 75 kN, and (c) interpass rolled using a profiled roller at 75 kN. Interpass rolling results in pronounced $\alpha$-lath refinement, increased lath fragmentation, and improved microstructural uniformity, with the profiled roller producing the most refined and homogeneous microstructure**

#### 4.1.3 Interpretation of Grain Growth Suppression

This microstructural evolution that was observed can be interpreted by one of the relationships that are temperature-dependent, β-grain growth:

$$d_\beta = k_0 t^n \exp\left( -\frac{Q}{RT}\right)$$

where $d_\beta$ is the β-grain size, $t$ is the time at elevated temperature, $Q$ is the activation energy for grain growth, $R$ is the gas constant, and $T$ is the absolute temperature.

Between-thermal-cycles in the as-deposited state have been shown to effectively lengthen the high-temperature exposure time, promoting β-grain coarsening. Interpass rolling brings stored strain energy which decreases the effective activation barrier of recrystallization, thus competing with thermally activated grain growth. This stress recrystallization breaks the β-grain coarsening despite frequent reheating, and the refined and isotropic microstructures are obtained.

**Table 1: Microstructural characteristics of WAAM Ti–6Al–4V under different rolling conditions**

| Sample ID | Roller Type | Rolling Load (kN) | Rolled Layers | Average $\alpha$-lath width (μm) | Prior β-grain size (μm) | $\alpha$ / β phase fraction (%) | Key microstructural observations |
|---|---|---|---|---|---|---|---|
| Control | — | 0 | — | 15–18 | 120–130 | 60 / 40 | Coarse columnar β grains, pronounced HAZ banding, strong anisotropy |
| R-P50 | Profiled | 50 | Last layer | 12–14 | 95–100 | 62 / 38 | Partial β-grain fragmentation, reduced $\alpha$-lath thickness |

| | | | | | | | |
|---|---|---|---|---|---|---|---|
| R-P75 | Profiled | 75 | Last layer | 10–12 | 80–85 | 63 / 37 | Significant recrystallization, refined $\alpha$-laths, minimal banding |
| R-F50 | Flat | 50 | Last layer | 13–15 | 100–105 | 61 / 39 | Moderate grain refinement, residual columnar features remain |
| R-F75 | Flat | 75 | Last layer | 11–13 | 90–95 | 62 / 38 | Improved refinement but less effective than profiled roller |

EBSD IPF analysis confirms further the disruption of continuity of the 2 -grain and inhibition of HAZ banding (Fig. 4a-c). Quantitative measurements **(Table 1)** confirm a systematic reduction in both $\alpha$-lath width and prior β-grain size with increasing rolling severity, with the profiled roller at 75 kN producing the smallest characteristic microstructural length scales.

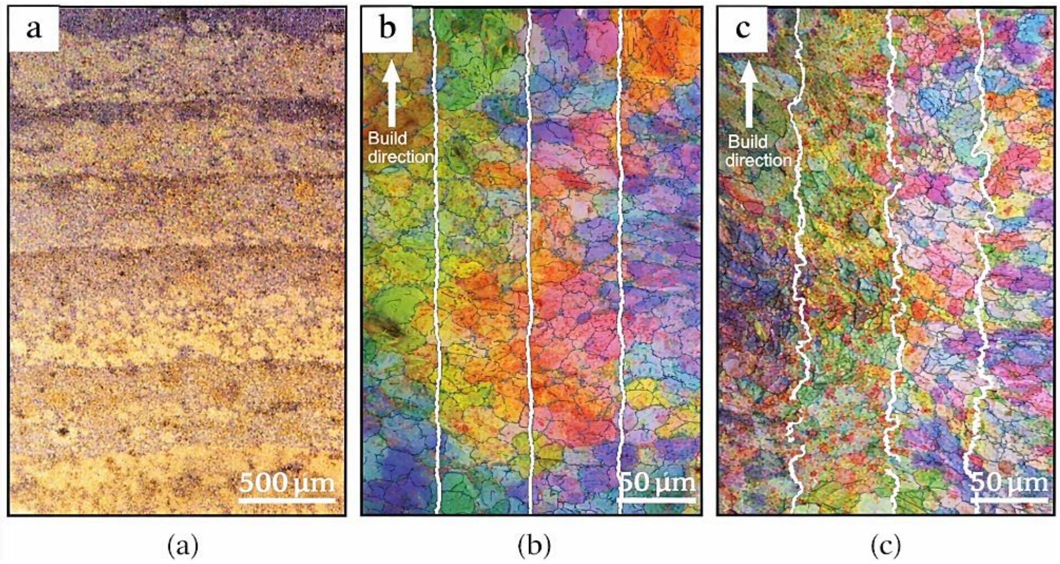


**Figure 4(a-c) Heat-affected zone (HAZ) banding and β-grain boundary evolution in WAAM Ti–6Al–4V. (a) Optical micrograph of the as-deposited wall showing pronounced HAZ banding arising from repeated thermal cycling during layer-by-layer deposition. (b) EBSD inverse pole figure (IPF) map of the unrolled condition, revealing coarse, columnar prior-β grains aligned along the build direction. (c) EBSD IPF map of the interpass rolled condition (profiled roller, 75 kN), demonstrating disruption of β-grain continuity, enhanced grain fragmentation, and reduced anisotropy. White dashed lines indicate representative β-grain boundaries and HAZ bands**

### 4.2 Mechanical Properties and Isotropy Enhancement

#### 4.2.1 Tensile Behaviour in Build and Transverse Directions

Interpass rolling was assessed in terms of mechanical performance in uniaxial tensile testing in the transverse (X) and build (Z) directions. Stress-strain curves at ambient temperature of as-deposited state (Fig. 5a) indicate that there is a great deal of anisotropy with the X-direction stress-strain curves displaying a stronger yield strength and ultimate tensile strength (UTS) than the Z-direction curves.

On the build direction, the as-deposited samples have a decrease of about 5-7 percent in yield strength and UTS (Table 2). This anisotropy is directly connected to the existence of columnar-shaped β grains that are parallel to the Z-direction which constrain the strain accommodation at the boundaries of layers and the early localization at the tensile loading.

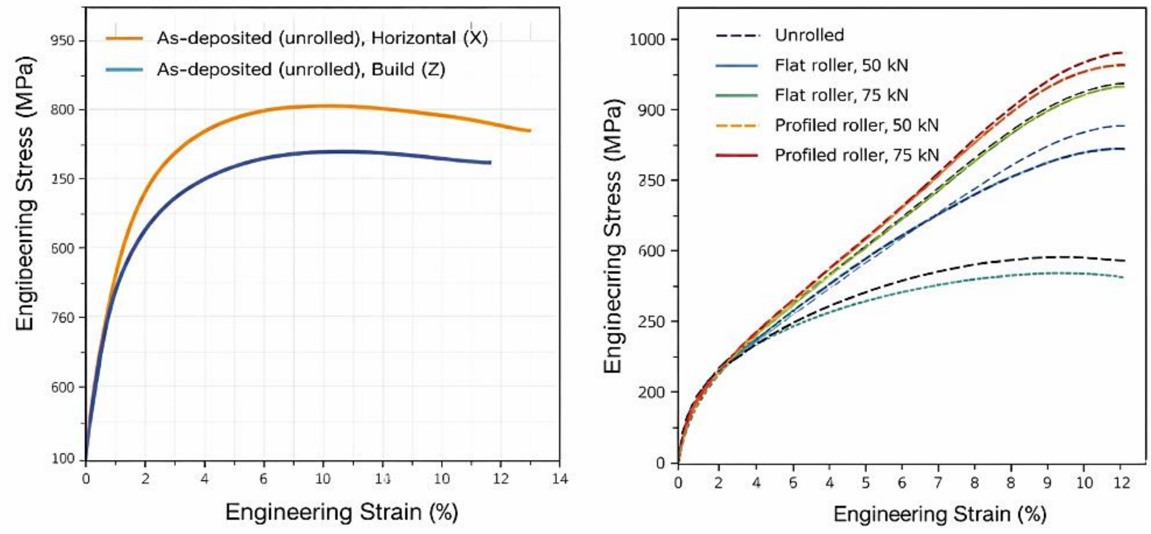


(a) (b)

**Figure 5(a-b). Engineering stress–strain behaviour of WAAM Ti–6Al–4V under different conditions. (a) Comparison of tensile response in horizontal (X) and build (Z) directions for the as-deposited (unrolled) condition, highlighting pronounced anisotropy. (b) Effect of interpass rolling load and roller geometry on tensile behaviour, showing enhanced strength, ductility, and strain-hardening response for rolled samples, with profiled rollers at 75 kN exhibiting the most significant improvement**

**Table 2: Mechanical properties of WAAM Ti–6Al–4V under different rolling conditions**

| Sample condition | Rolling load (kN) | Test direction | Yield strength (MPa) | Ultimate tensile strength (MPa) | Elongation (%) | Remarks |
|---|---|---|---|---|---|---|
| As-deposited (Unrolled) | 0 | X (Horizontal) | 880 ± 15 | 920 ± 20 | 12 ± 0.5 | Pronounced anisotropy |
| As-deposited | 0 | Z (Build) | 845 ± 15 | 885 ± 20 | 10 ± 0.5 | Columnar β-grain |

| | | | | | | |
|---|---|---|---|---|---|---|
| (Unrolled) | | | | | | dominated |
| Flat roller | 50 | X (Horizontal) | 915 ± 18 | 960 ± 22 | 13 ± 0.6 | Partial isotropy improvement |
| Flat roller | 50 | Z (Build) | 890 ± 18 | 935 ± 22 | 12 ± 0.6 | Reduced grain size |
| Flat roller | 75 | X (Horizontal) | 930 ± 15 | 980 ± 18 | 14 ± 0.5 | Improved strength |
| Flat roller | 75 | Z (Build) | 910 ± 15 | 960 ± 18 | 13 ± 0.5 | Reduced anisotropy |
| Profiled roller | 75 | X (Horizontal) | 940 ± 12 | 995 ± 15 | 15 ± 0.4 | Near-isotropic behavior |
| Profiled roller | 75 | Z (Build) | 932 ± 12 | 987 ± 15 | 15 ± 0.4 | Best mechanical balance |

#### 4.2.2 Effect of Rolling Load and Roller Geometry on Strength and Ductility

Interpass rolling leads to a uniform enhancement in the mechanical properties in both directions of loading (Fig. 5b). When the rolling load is increased by 25 kN to 75 kN, yield strength and UTS are increased progressively with better elongation.

The largest improvement is seen with samples rolling on a profiled roller with a 75kN force. In this state UTS values are inclined to be close to ~980–995 Mpa in X and Z directions with an elongation of about ~15%. This is equivalent to an increase in strength of about 68-8 percent and a 20-25% increase in ductility (Table 2).

Comparison of a roller geometry directly reveals that profiled rollers perform better than flat rollers at the same load. This is due to the enhanced performance of the 600 series with better β-grain fragmentation and $\alpha$-lath refining, which is typical of the increased localized plastic strain and better distribution of strain during rolling.

#### 4.2.3 Mechanical Isotropy and Deformation Behaviour

The extent of mechanical anisotropy was determined as the difference between tensile strengths of X- and Z- directions. Interpass rolling, as can be seen in Fig. 6, has a potent effect in reducing this difference. Although an anisotropy of about 35 MPa is observed with the unrolled condition a region of 75 kN rolling decreases the anisotropy to less than 10 Mpa with profiled roller achieving an almost isotopic behaviour (less than 1% of difference in UTS).

The initial slopes of elasticity of rolled specimens are steeper and the strain-hardening behaviour is better than that of unrolled samples. These higher yield strengths are due to grain boundary strengthening and $\alpha$-lath refinement and the higher ductility is due to a higher homogeneous dislocation slip in refined and equiaxed structures of β-grain. Large columnar grains are suppressed and this eliminates strain incompatibility between layers, delaying necking and increasing build-direction ductility.

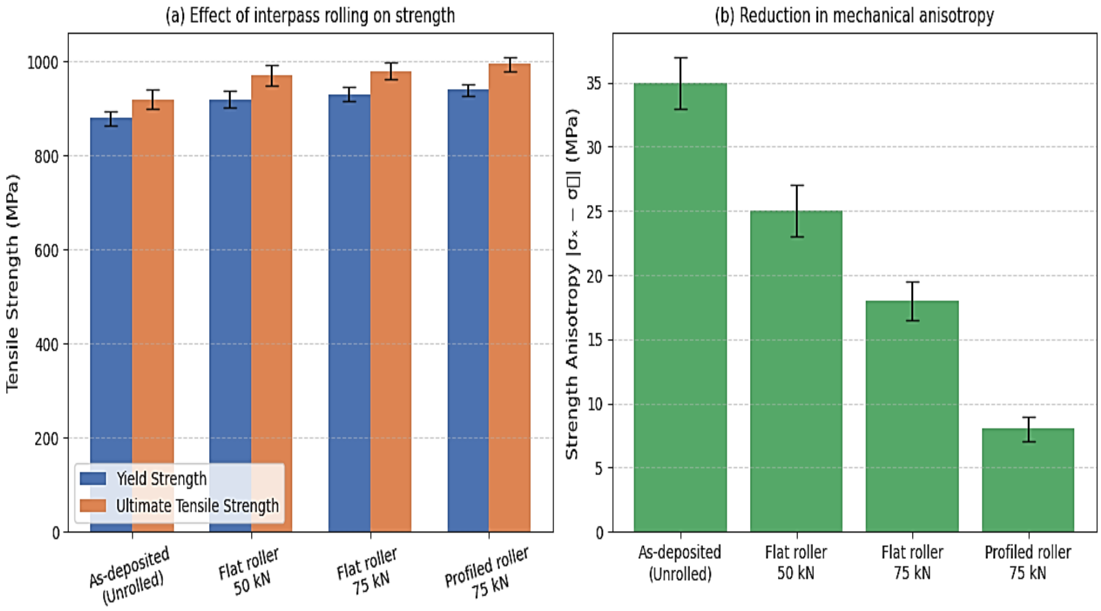


**Figure 6. Effect of interpass rolling on mechanical isotropy of WAAM Ti–6Al–4V. (a) Comparison of yield strength and ultimate tensile strength for as-deposited and rolled samples under different rolling loads and roller geometries. (b) Strength anisotropy quantified as the absolute difference between tensile strengths measured along the build (Z) and transverse (X) directions**

## 5. DISCUSSION

### Microstructure Control through Interpass Rolling

As the findings show, interpass rolling essentially changes solidification-based microstructure which is characteristic of WAAM Ti-6Al-4V. The β-grains formed during continuous epitaxial growth of pervi-betra grains along the built direction form long columnar grains and strong banding of the heat effected zone (HAZ). This microstructural heterogeneity is in line with the severe thermal gradients and periodic reheating inherent to arc-based additive manufacturing.

In interpass rolling, plastic deformation is performed in a controlled way among the thermally active deposited layers leading to storing up of plastic strain energy. In later thermal cycles, this strain facilitates strain-assisted recrystallization, competing with thermally driven β-grain coarsening. This causes β-grain continuity to be broken and the effective grain size to be lowered about 20-25% and especially at elevated rolling loads. Reduction in $\alpha$-lath width to approximately 10 μm (observed) further suggests a high density of nucleation in the course of $\alpha$ precipitation which is caused by the fined β-grain structure and high density of defects.

Another advantage of interpass rolling is indicated by the inhibition of HAZ banding in rolled samples. Through altering the thermal-mechanical history of each individual deposition, rolling can be used to decrease the microstructural distinction between moves in a deposition map, resulting in a less discontinuous microstructure across the build height. This is more significant when the profiled roller is used, which leads to greater local strain on the plastic than the flat roller with the same nominal load.

### Influence of Rolling Load and Roller Geometry

Rolling load and roller geometry are both very important in the level of microstructural refinement. A progressive increase in rolling load, between 50 and 75 kN, is known to improve β-grain fragmentation and $\alpha$-lath refining, suggesting the existence of a level of plastic strain at which effective recrystallization is utilized in further heat treatment. This premature failure at 100 kN implies that the accumulation of strain is beyond the ductile nature of the thermally softened material creating a maximum processing limit to in-situ rolling.

The higher performance of the profiled roller compared to the flat roller can be explained by the fact that the profiled roller has a non-uniform contact geometry, and thus it concentrates deformation at the lower side of the roller profile and enhances the depth of penetration of effective strain. This strain distribution has the advantage of encouraging a uniform recrystallization throughout the deposited layer resulting in a more uniform grain structure and minimized anisotropy of microstructure.

**Mechanical Isotropy Enhancement**

The observed microstructural evolution is directly reflected in the mechanical response. The raw material of the WAAM is highly anisotropic in tensile properties, whereby the strength and ductility increases in the direction of the build with poor compatibility of strain across columnar β-grains and inter-layer planes. Interpass rolling is a great way of alleviating such behavior by sharpening grain structure and morphological texture.

The difference in the strength of both the X and Z directions is reduced to less than ~35 MPa to less than 10 MPa, which is almost isotopic in its mechanical behavior. The concomitant increase in strength, as well as elongation, is an indication that interpass rolling does not only refine the strength, but also improves the strain accommodation through more uniform slip activation between refined and equiaxed micro-characteristics.

These three synergistic processes can hence be said to be behind the decrease in anisotropy: (i) columnar β-grains fragmentation, (ii) morphological refinement of $\alpha$-lathes, and (iii) inhibition of the banding of the HAZ. All these aspects increase the strain localization, necking delay, and enhance inter-layered load transfer, leading to mechanical reliability.

**Implications for WAAM Process Design**

In contrast to post-deposition heat treatment or hot forging, interpass rolling does not cause any problem with the WAAM process chain and does not involve any special high-temperature treatment and complicated tooling. The current findings have shown interpass rolling to be a viable solution to one of the most problematic constraints of WAAM, which is mechanical anisotropy, without losing the benefits of the process, in terms of deposition rate and geometric flexibility.

## 6. CONCLUSION

The research indicates that interpass rolling is a practical in-situ process to refine microstructures and improve mechanical isotropy of Ti-6Al-4V produced by WAAM. Its main findings are the following:

1. Refinement at the microstructure level: Interpass rolling decreases previous β grain size by approximately 20-25 percent and narrows $\alpha$-lath width to about 10, which is the largest refinement of all made with a profile roller and a rolling load of 75 kN.
2. Smearing of microstructural heterogeneity: Rolling interrupts columnar continuity of β -grains and is followed by a significant decrease in banding of heat-sensitive zones, and the microstructural homogeneity along the build direction is enhanced.
3. Mechanical performance improvement: Interpass rolling improves tensile anisotropy (reduction of tensile anisotropy in the un rolled material is about ~35 MPa) to tensile anisotropy of less than 10 MPa in the optimally rolled material). Interpass rolling also improves tensile ductility in both the build and transverse directions.

4. Rolling parameter role: It is well known that increased rolling loads and profiled roller geometry are more successful in straining-assisted recrystallization and obtaining near-isotopic mechanical behavior; however, at too large rolling loads, there is premature failure.

## 7. REFERENCES


[1]. Lei, Z., Gao, P., Wang, X., Zhan, M., & Li, H. (2021). Analysis of anisotropy mechanism in the mechanical property of titanium alloy tube formed through hot flow forming. *Journal of Materials Science & Technology*, *86*, 77–90. https://doi.org/10.1016/j.jmst.2021.01.038

[2]. Maurya, A. K., Yeom, J.-T., Kang, S. W., Park, C. H., Hong, J.-K., & Reddy, N. S. (2022). Optimization of hybrid manufacturing process combining forging and wire-arc additive manufactured Ti-6Al-4V through hot deformation characterization. *Journal of Alloys and Compounds*, *894*, 162453. https://doi.org/10.1016/j.jallcom.2021.162453

[3]. Mu, H., He, F., Yuan, L., Commins, P., Wang, H., & Pan, Z. (2023). Toward a smart wire arc additive manufacturing system: A review on current developments and a framework of digital twin. *Journal of Manufacturing Systems*, *67*, 174–189. https://doi.org/10.1016/j.jmsy.2023.01.012

[4]. Narayana, P. L., Kim, J. H., Lee, J., Choi, S.-W., Lee, S., Park, C. H., Yeom, J.-T., Reddy, N. G. S., & Hong, J.-K. (2021). Optimization of process parameters for direct energy deposited Ti-6Al-4V alloy using neural networks. *The International Journal of Advanced Manufacturing Technology*, *114*(11–12), 3269–3283. https://doi.org/10.1007/s00170-021-07115-1

[5]. Narra, S. P., Cunningham, R., Beuth, J., & Rollett, A. D. (2018). Location specific solidification microstructure control in electron beam melting of Ti-6Al-4V. *Additive Manufacturing*, *19*, 160–166. https://doi.org/10.1016/j.addma.2017.10.003

[6]. Martina, F., Colegrove, P. A., Williams, S. W., & Meyer, J. (2015). Microstructure of interpass rolled wire + arc additive manufacturing Ti-6Al-4V components. Metallurgical and Materials Transactions A, 46, 6103–6118. https://doi.org/10.1007/s11661-015-3172-1

[7]. McAndrew, A. R., Rosales, M. A., Colegrove, P. A., Hönnige, J. R., Ho, A., Fayolle, R., … Prangnell, P. B. (2018). Interpass rolling of Ti-6Al-4V wire + arc additively manufactured features for microstructural refinement. Additive Manufacturing, 21, 340–349. https://doi.org/10.1016/j.addma.2018.03.006

[8]. Davis, A. E., Hönnige, J. R., Martina, F., & Prangnell, P. B. (2020). Quantification of strain fields and grain refinement in Ti-6Al-4V inter-pass rolled wire-arc AM by EBSD misorientation analysis. Materials Characterization, 170, 110673.https://doi.org/10.1016/j.matchar.2020.110673

[9]. Lunt, D., Ho, A., Davis, A., Martina, F., Hönnige, J., Quinta da Fonseca, J., & Prangnell, P. (2020). Microscopic strain localisation in WAAM Ti-6Al-4V during uniaxial tensile loading. MATEC Web of Conferences, 321, 03008.https://doi.org/10.1051/matecconf/202032103008

[10]. Donoghue, J., Davis, A. E., Daniel, C. S., Garner, A., Martina, F., Quinta da Fonseca, J., & Prangnell, P. B. (2020). On the observation of annealing twins during simulating β-grain refinement in Ti-6Al-4V high deposition rate AM with in-process deformation. Acta Materialia, 186, 229–241.

https://doi.org/10.1016/j.actamat.2020.01.009
[11]. Pan, Z., Zhang, H., Song, X., Wang, G., Wu, C., & Liu, X. (2022). Influence of micro-rolling on the strength and ductility of plasma-arc additively manufactured Ti–6Al–4V alloys. Journal of Materials Research and Technology, 21, 465–473. https://doi.org/10.1016/j.jmrt.2022.09.035
[12]. Xian, G., Pan, J., Lee, J., & Kang, N. (2024). Weakening the anisotropic property and refining prior-β grains via hammer peening treatment during wire arc additively manufacturing of Ti-6Al-4V. Metals, 14(11), 1261. https://doi.org/10.3390/met14111261
[13]. Kennedy, J. R., Davis, A. E., Caballero, A. E., Williams, S., Pickering, E. J., & Prangnell, P. B. (2021). The potential for grain refinement of wire-arc additively manufactured Ti-6Al-4V by ZrN and TiN inoculation. Additive Manufacturing, 40, 101928. https://doi.org/10.1016/j.addma.2021.101928
[14]. Zou, Z., Simonelli, M., Katrib, J., Dimitrakis, G., & Hague, R. (2020). Refinement of the grain structure of additive manufactured titanium alloys via epitaxial recrystallization enabled by rapid heat treatment. Scripta Materialia, 180, 66–70. https://doi.org/10.1016/j.scriptamat.2020.01.027
[15]. Feng, Y., Jiang, Q., He, W., Zhang, G., & Fan, D. (2025). Effects of arc mode on morphology, microstructure and mechanical properties of titanium alloy wire arc additive manufacturing. *Journal of Materials Research and Technology*, *36*, 1–15. https://doi.org/10.1016/j.jmrt.2025.03.294
[16]. Kennedy, J. R., Davis, A. E., Caballero, A. E., White, M., Fellowes, J., Pickering, E. J., & Prangnell, P. B. (2021). Microstructure transition gradients in titanium dissimilar alloy (Ti–5Al–5V–5Mo–3Cr/Ti–6Al–4V) tailored wire-arc additively manufactured components. *Materials Characterization*, *182*, 111577. https://doi.org/10.1016/j.matchar.2021.111577
[17]. Liu, J., Zhang, K., Bermingham, M. J., Fraser, H. L., Hodgson, P., Heilmaier, M., Boretti, A., Zhu, Y., & Huang, A. (2026). Fatigue and damage tolerance performance of additively manufactured titanium alloys for structural applications: A comprehensive review. *Materials Science and Engineering: R: Reports*, *167*, 101135. https://doi.org/10.1016/j.mser.2025.101135
[18]. Lu, F., Ma, Q., Liu, E., Wei, R., Bai, J., Gao, Q., & Qi, J. (2025). Advancements in understanding the microstructure and properties of additive manufacturing Ti–6Al–4V alloy: A comprehensive review. *Journal of Alloys and Compounds*, *1027*, 180543. https://doi.org/10.1016/j.jallcom.2025.180543
[19]. DebRoy, T., Wei, H. L., Zuback, J. S., Mukherjee, T., Elmer, J. W., Milewski, J. O., Beese, A. M., Wilson-Heid, A., De, A., & Zhang, W. (2018). Additive manufacturing of metallic components – Process, structure and properties. *Progress in Materials Science*, *92*, 112–224. https://doi.org/10.1016/j.pmatsci.2017.10.001

***Conflict of Interest Statement:*** *The authors declare that there is no conflict of interest regarding the publication of this paper.*

***Generative AI Statement:*** *The authors confirm that no Generative AI tools were used in the preparation or writing of this article.*

***Publishers Note:*** *All statements made in this article are the sole responsibility of the authors and do not necessarily reflect the views of their affiliated institutions, the publisher, editors, or reviewers. Any products mentioned or claims made by manufacturers are not guaranteed or endorsed by the publisher.*



***Cite this Article***

Anil Sharma, Dr. Alok Choudhary. Microstructure Refinement and Mechanical Isotropy Enhancement in WAAM Ti–6Al–4V via Interpass Rolling. International Research Journal of Engineering & Applied Sciences (IRJEAS). 14(1), pp. 29-44, 2026. https://doi.org/10.55083/irjeas.2026.v14i01004